Rev.Adv.Mater.Sci. 4 (2003) 48-54

UV ENHANCEMENT OF THE GAS SENSING PROPERTIES OF NANO-TiO_2

Tsung-Yeh Yang[1], Hong-Ming Lin[1], Bee-Yu Wei[1], Chuan-Yi Wu[1] and Chung-Kwei Lin[2]

[1]Department of Materials Engineering, Tatung University, Taipei 104, Taiwan, R.O.C.
[2]Department of Materials Science, Feng Chia University, Taichung 407, Taiwan, R.O.C.

Received: January 21, 2003

Abstract. In this study, the gas-sensing properties of nanocrystalline TiO_2 are enhanced by submitting the sensor system to UV light irradiation. TiO_2 gas sensing material based on nanosized particles is produced by gas condensation method. The crystal structure and ceramic microstructure of the powders are determined by TEM and XRD. Structural and morphological studies as well as UV irradiation are carried out in order to investigate their influence on the sensing properties of TiO_2 sensor. The sensitivity of the TiO_2 sensor is affected by the presence of O_2^- or O^- on the TiO_2 surface that is enhanced by the photocatalytic effect. Gaseous CO is detected under UV light illumination. The results indicate that the sensing properties of TiO_2 are affected by the wavelength and the intensity of the UV light. The photocatalytic activity enhances the sensitivity of the nano-TiO_2 sensors by more than 30 times.

1. INTRODUCTION

Nanocrystalline (NC) materials, exhibiting small particle size and large surface area, can be used for gas sensors which require an excellent surface effect. Metal oxide semiconductors (MOS) materials, such as ZnO, SnO_2, WO_3, and TiO_2 etc., are reported to be usable as semiconductor gas sensors. These candidates have non-stoichiometric structures, so free electrons originating from oxygen vacancies contribute to the electronic conductivity [1]. The demand for accurate and dedicated sensors that will be able to provide precise process control and automation in manufacturing process, and also to monitor and control environmental pollution, have accelerated the development of new sensing materials and sensors technology over the last decade [2,3]. There are several challenges that need to be achieved in developing gas sensors for harsh industrial environments. Operation at temperatures greater that 500 °C requires materials that are thermally stable. In addition, sensors must have physicochemical features that promote both sensitivity and selectivity. In presence of multiple reducing gases, a selective sensor must be able to distinguish between the different gases, or at the very least, respond to only one of the gases in the mixture [4]. Some new types of sensing materials are still being studied and exploited at present time. The most extensively studied ceramic gas sensor is based on SnO_2 and is routinely used for low temperature applications [5]. The addition of dopants to metal oxide semiconductors is the most common route for obtaining selective gas sensors, e.g. the presence of Pd and Pt enhances the CO selectivity of SnO_2 sensors [6]. In 1990, a Nb_2O_5 doped TiO_2-based sensor for humidity was investigated by Katayama [7]. At the same time, Hara et al. [8] developed a semiconductor pH sensor using a Nb_2O_5-doped TiO_2 single crystal as a pH-sensitive electrode for use in high-temperature aqueous solutions up to 250 °C. In 1993, Takao et al. [9] determined fish freshness, which decreases with the increase of $(CH_3)N_3$ (TMA) concentration, with Ru-doped TiO_2. Lin *et al*. [10] synthesized NC TiO_2 by means of the gas-condensation method as a sensing material, and a maximum sensitivity of about 70 was reached under 250 ppm H_2S/Air mixture at 500 °C. In 1997, Lin et al. [11] doped nanocrystalline (NC) TiO_2 with

Corresponding author: Hong-Ming Lin, e-mail: hmlin@ttu.edu.tw

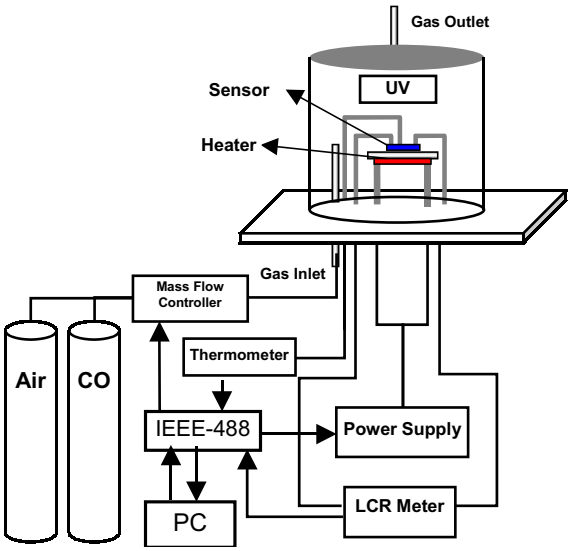

Fig. 1. Scheme of the measuring setup.

NC Pt to improve the sensitivity and response time of the sensors. NC TiO_2 and NC Pt /TiO_2 sensors were compared by examining the relationship between the operation temperature and sensitivity to CO and NO_2 gases. The optimal operation temperature for NO_2 and CO gases was about 190 °C for the NC TiO_2 sensor and about 170°C for the NC Pt/TiO_2 sensor. A maximum sensitivity of about 14 for the NC TiO_2 sensor was observed under 100 ppm gaseous NO_2 and the response time was about 1-3 minutes. In 1999, Carotta *et al*. [12] fabricated thick films of nanostructured TiO_2 and niobium-doped TiO_2. They proved that TiO_2-based thick film sensors exhibit a suitable sensitivity to atmospheric environmental monitoring provided that the microstructural properties of the materials were suitably correlated to the required electrical features. In 2001, Savage [13] examined the anatase form of TiO_2 for CO and CH_4 sensing at 600 °C. At the same time, the n-p semiconducting titanium oxides composite was used as gas sensor for CO and CH_4 sensing at 600 °C [14]. A selective response to CO was obtained at 600 °C although it was a n-type response. According to the newest report publish by Ruiz *et al*. [15], platinum supported on titania was prepared by two impregnation procedures using platinum chloride as a precursor. Anatase surface reactivity towards platinum was higher than rutile since better catalytic incorporation has been observed.

However, there are scarce reports on the enhancement of the gas-sensing properties by photostimulation. In a photocatalytic system, photo-induced molecular transformation or reaction takes place at the surface of catalyst [16]. A basic mechanism of photocatalytic reaction on the generation of electron-hole pairs is as follows: when a photocatalyst is illuminated by a light whose corresponding energy is larger than the band gab energy, electron-hole pairs diffuse out of the surface of the photocatalyst and participate in the chemical reaction with electron donor and acceptor. To achieve a higher photoactivity, it is essential to suppress the subsequent recombination process and to increase the lifetime of separated electron-hole pairs, so that fast electron transfer occurs from the surface to the adsorbed intermediates. There are many variables that affect the photoactivity such as particle size, crystal structure, and incident light intensity. [17-22]. This photocatalytic effect will change the surface properties of sensing materials. In this study, the gas-sensing properties of nano-TiO_2 under UV illumination are examined.

2. EXPERIMENTAL

Alumina substrates (0.63 mm thick) with gold electrodes and an Ag-Pt heater printed on both sides are used in this study. A tantalum boat is used as a resistance-heating source for Ti evaporation under 5-mbar of helium. NC Ti particles are directly coated on the surface of Au electrodes, and pure oxygen is back-filled into the chamber to form NC TiO_2. Then, a step-heating process up to 600 °C is performed to strength the bonding properties of the nano-TiO_2 porous sensing film. The step-heating process not only enhances the adhesion between the substrate and NC TiO_2, but also maintains the porous network-like structure of NC TiO_2, thus increasing the sensing area. On another hand, annealing at temperatures above 600 °C will crash the porous film as a result of the intensive chemical interaction of NC TiO_2 with the electrode material and the substrate. The sample is examined in a chamber with the detecting gases flowing through. A mass flow controller controls the detecting gases at a flow rate of 500 square cubic centimeter per minute (SCCM) and maintains a dynamic equilibrium. The Ag-Pt heater is used to heat and control the operation temperature of sensors.

The detecting system is linked to the computer with an IEEE-488 interface to adjust the system parameters and record the data. The electrical properties of sensor are measured at various temperatures from room temperature up to 300 °C, and at various concentrations of gaseous CO (80-300 ppm CO diluted in dry air) with or without UV illumination. The initial electrical characteristics of the gas sensor are stabilized in dry air for at least 1 hour

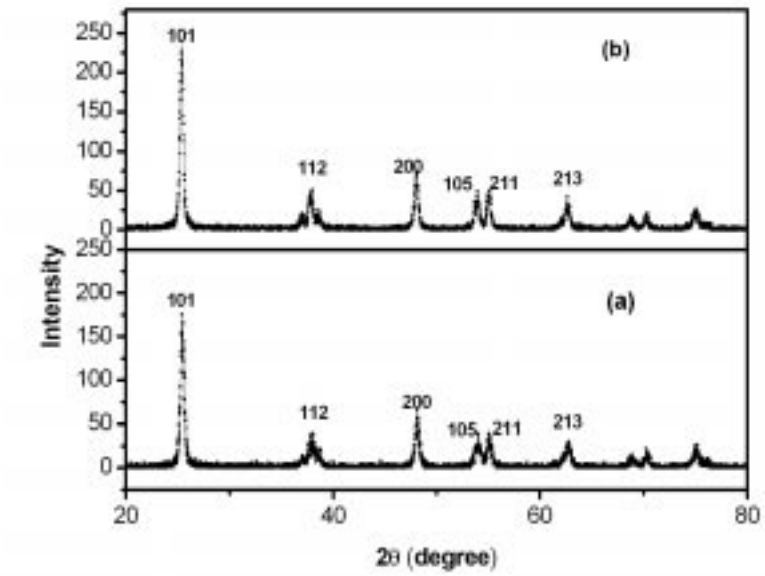

Fig. 2. X-ray diffraction patterns of TiO_2 nanoparticles (a) as prepared (anatase phase) and (b) after sintering at 600 °C for 2 hours (still anatase phase).

before any test gas exposure. The relative changes in the electrical parameters of the film are considered as sensor output. The set-up of the measuring system is described in Fig. 1. Son King UV light (model SKUVL-100) with a wavelength of 368 nm and a power of 3.25±1 mW/cm^2 is used in this study. The distance between the UV light and the sample is one centimeter.

3. RESULTS AND DISCUSSION

TiO_2 nanoparticles are produced by gas condensation technique under 5-mbar of helium. The powder X-ray diffraction (XRD) spectrum shown in Fig. 2a confirms that the as-prepared sample is purely anatase. Upon heating at 600 °C for 2 hours, it is still in the anatase form, as seen in the XRD spectrum (Fig. 2b). Fig. 3 (a) and (b) show the TEM images of as-prepared nano TiO_2 and after the heat treatment at 600 °C for two hours, respectively. There is no obvious particle growth. Fig. 3(c) is the diffraction pattern corresponding to Fig. 3(b) and reveals that the anatase structure is not changed after sintering at 600 °C. The size distribution of the nano TiO_2 particles is measured from TEM images and shown in Fig. 4. The mean particle size is about 7.2 nm and 13.7 nm for as prepared sample and after the heat treatment, respectively. The sintering causes the increase of the mean particle size, but also strengthens the bonding properties between nano TiO_2 and the alumina substrate. Fig. 5 (a) and (b) show the SEM micrographs of the as-prepared and sintered nano TiO_2 samples.

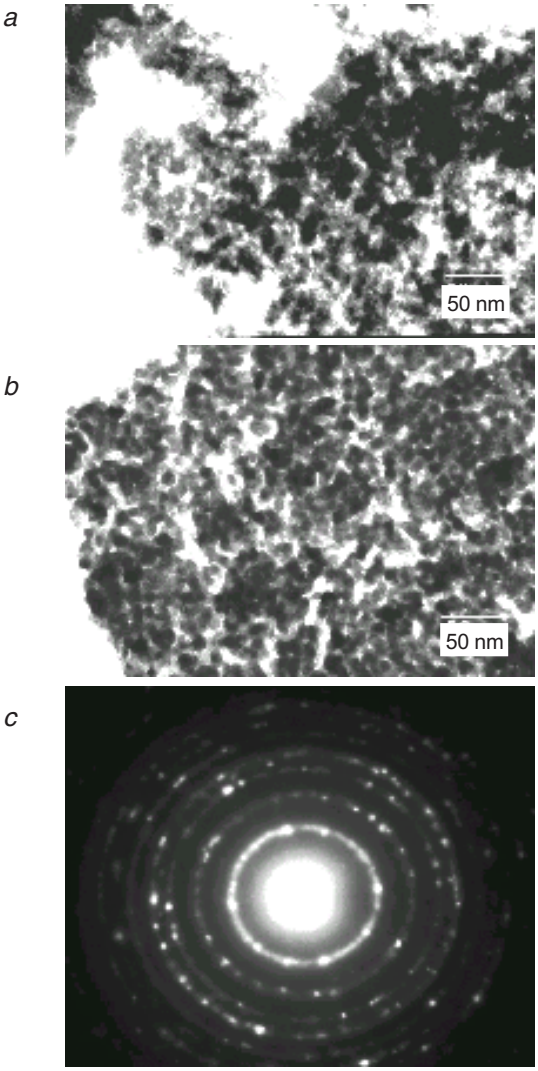

Fig. 3. TEM images of nano TiO_2, (a) as-prepared, (b) after sintering at 600 °C for 2 hours, and (c) diffraction pattern corresponding to (b) and showing the anatase structure.

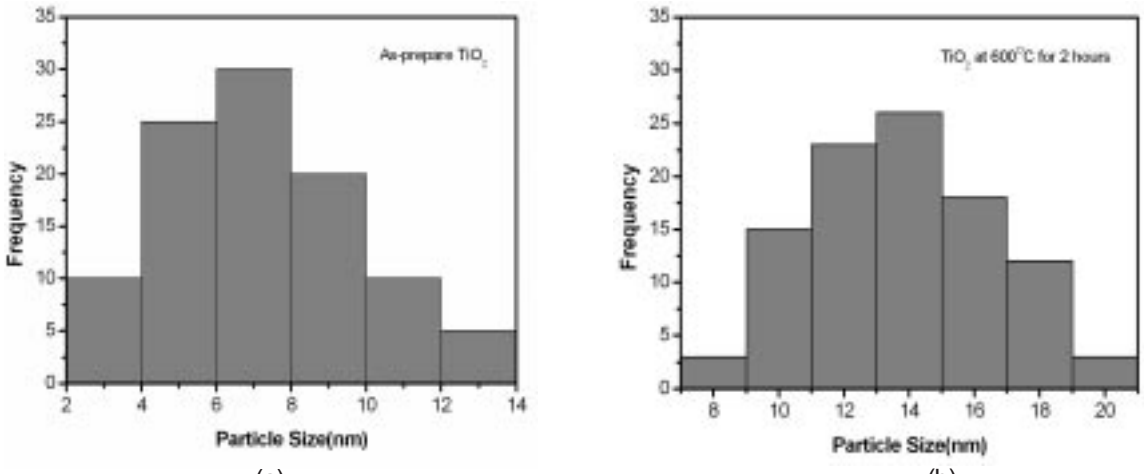

(a) (b)

Fig. 4. Particle size distribution of NC TiO_2 (a) as-prepared (mean particle size about 7.2 nm) and (b) sintered at 600 °C for 2 hours (mean particle size about 13.7 nm).

Fig. 6 shows the resistance-temperature curves for the NC TiO_2-based sensor in air and in 100 ppm of gaseous CO with or without UV irradiation. The results indicate that UV illumination enhances the n-type behavior of nano TiO_2 and increases the sensitivity to CO. In dry air, the resistance increases under UV irradiation. This indicates the increase of ionized O_2^- or O^- species, thus contributing to increase the depletion of the surface layer. Therefore, an increase of the thickness of depletion layer under UV irradiation leads to a resistance increase as shown in Fig. 6.

The sensitivity of nano TiO_2 sensor towards different concentrations of gaseous CO without or with UV enhancement are shown in Fig. 7(a) and (b). Under UV irradiation, the sensitivity to 300 ppm CO can be increased by a factor of 10. The sensitivity to 300 ppm CO is 2.51 and 87 without and with UV irradiation, respectively. The optimal operation temperatures are about 115 °C and 220 °C with and without UV irradiation, respectively. Also, a second sensitivity maximum is observed at a higher temperature (about 200 °C) when the sample is not UV irradiated. It seems that the UV light stimulates the surface defects and enhances the catalytic properties at about 200 °C, thus leading to a dramatic increase the gas sensing properties.

If the sensitivity is plotted as a function of the CO concentration, the difference between the UV irradiated sample and the non-irradiated sample is significant as shown in Fig. 8. Without UV illumination, the change in the sensitivity is about 0.03/10 ppm of CO. In the case of UV enhancement, the change in the sensitivity is about 1.4/10 ppm in

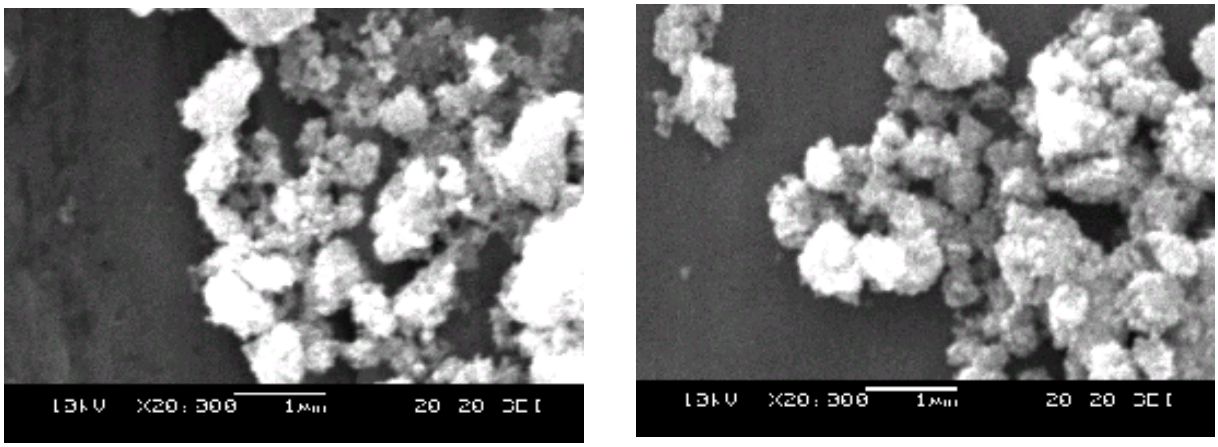

(a) (b)

Fig. 5. SEM micrographs of nano-TiO2 (a) as-prepared and (b) after sintering at 600 °C for 2 hours.

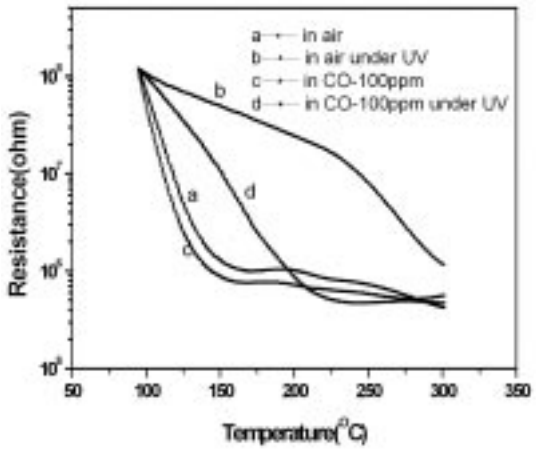

Fig. 6. Electric response at 100 ppm CO of nano-TiO_2 with and without UV illumination.

80-200 ppm CO range and about 5.3/10 ppm between 200 and 300 ppm of CO. Under UV irradiation, the sensitivity is increased by a factor of 170.

In nanocrystalline TiO_2, the electron concentration depends on the deviations of the composition from the non-stoichiometry caused by oxygen vacancies (V_o), which are predominant atomic defects. Also, the electrical properties of nanocrystalline TiO_2 strongly depend on the surface states produced by the chemisorption of oxygen and other gaseous molecules, resulting in space charge and electron barriers. CO is a reducing gas that interacts with chemisorbed oxygen species (O_2^-, O^-, O^{2-}) leading to an increase of the electron concentration in the conduction band. Depending on the temperature range, there are different adsorbed oxygen species that all affect the surface space charge layer of nano TiO_2 [23]. At temperature below 150 °C, oxygen is adsorbed as O_2^- molecular-ionic species at the surface of TiO_2 as shows in Eqs. (1) and (2). When the temperature varies from 150 to 400 °C, the O^- atomic-ionic species adsorb at the TiO_2 surface according to Eq. (3). If there is no reducing gas in the system, O_2^- and O^- oxygen species withdraw electrons from the TiO_2 surface, thus causing a resistance increase of TiO_2. When a reducing gas like CO is introduced, it reacts with the surface oxygen species according to the reactions shown in Eqs. (4) and (5) and depending on the temperature range.

$$TiO_2 + O_{2(g)} = O_2(\text{phys}), \quad (1)$$

$$O_2(\text{phys}) + \bar{e} = O_2^- \text{ molecular-ionic species}, \quad (2)$$

$$O_2^- + \bar{e} = 2O^- \quad \text{atomic-ionic species}, \quad (3)$$

$$2CO + O_2^- = 2CO_2 + \bar{e} \quad T < 150\ °C, \quad (4)$$

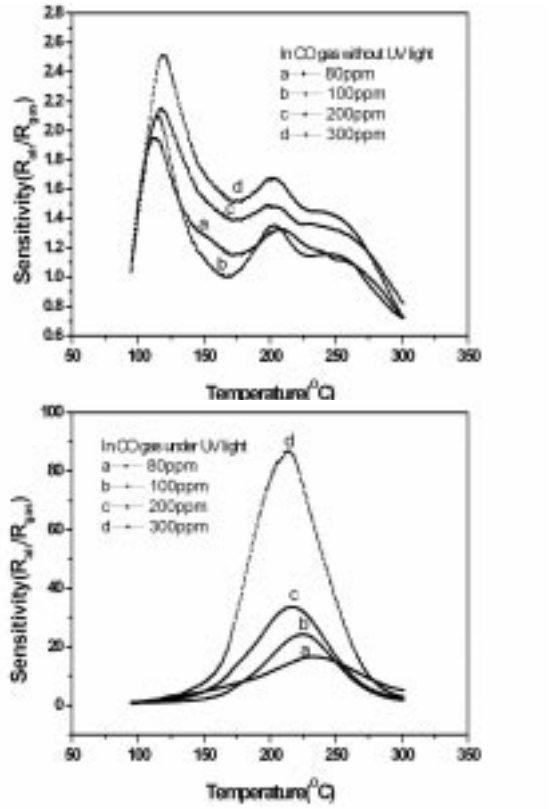

Fig. 7. Sensitivity of the nano-TiO_2 sensor (a) without and (b) with UV illumination at different CO concentrations.

$$CO + O^- = CO_2 + \bar{e} \quad 150\ °C < T < 400\ °C. \quad (5)$$

Under UV irradiation, $\bar{e}$-h^+ pairs can be generated at the TiO_2 surface by the absorption of UV light. This effect is illustrated Fig. 9(a) and (b). Following electronic excitation, the major process occurring at the surface of NC TiO_2 is the reduction of electron acceptor O_2^- by photo generated electrons, that is $O_2^- + e^- = 2O^-$. For an n-type semiconductor oxide, the

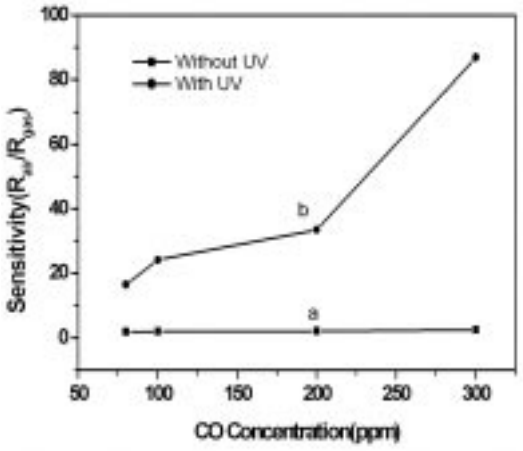

Fig. 8. Sensitivity as function of CO concentrations with or without UV illumination.

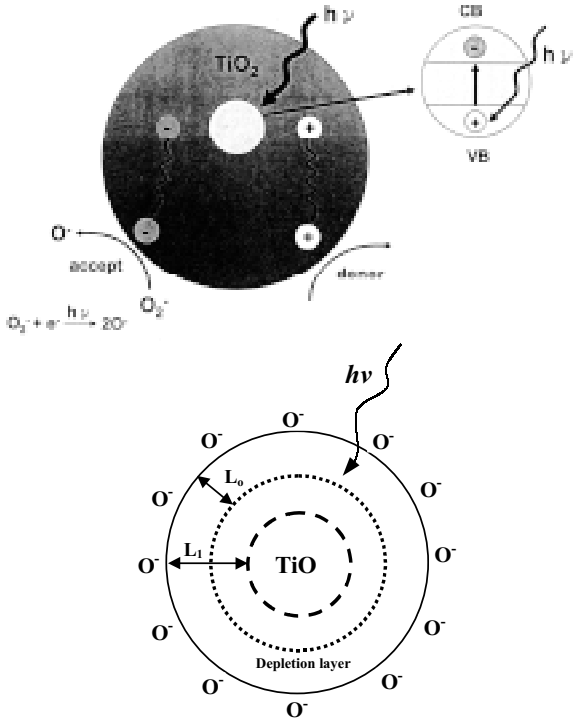

Fig. 9. Illustration of the major processes occurring on an NC TiO_2 following electronic excitation. (a) At the surface of NC TiO_2, photo-generated electrons can reduce an electron acceptor O_2^- and (b) adsorption decreases the charge carrier density at the interface.

adsorption decreases the charge carrier density at the interface and increases the depletion region as shown in Fig. 9(b). Without UV irradiation, the thickness of depletion layer is L_o and increases to L_1 when the sample is UV irradiated. The absorption of the UV light increases the density of ionic oxygen at the nano TiO_2 surface, thus providing more active sites for further reaction with CO. The result of the UV irradiation is experimentally observed in Fig. 6. TiO_2 is well known as a good candidate material for photocatalysis and gas sensing. A basic mechanism of photocatalytic reaction is the generation of electron-hole pairs by UV light. The photocatalytic reaction dramatically affects the gas-sensing properties as it changes the surface activity.

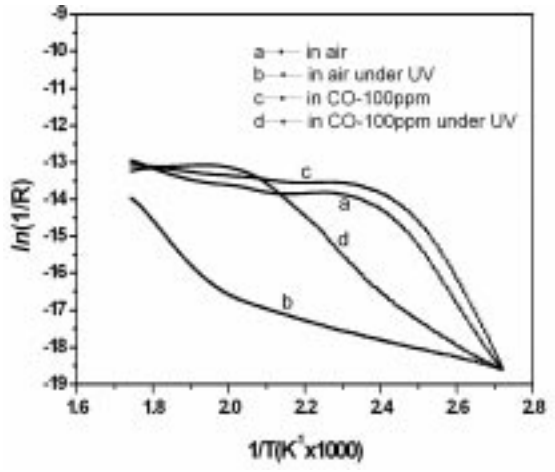

Fig. 10. ln(1/*R*) versus 1/*T* at 100 ppm CO.

To examine the surface activity of TiO_2, the results of Fig. 6 are plotted in a different way: ln(1/*R*) versus 1/*T* (Fig. 10) and the Arrhenius relationship is considered as follows:

$$\ln(1/R) = \ln(1/R_o) - E_a/kT, \quad (6)$$

where *R* is the resistance of the sensor at constant CO concentration, R_o is a constant, *k* is the Plank's constant, *T* is the temperature in *K*, and E_a is the activation energy (eV) of the surface reaction. The results are listed in Table 1. In dry air, the activation energy varies from 0.35 eV without UV irradiation to 0.05 eV with UV stimulation. The activation energy for gaseous CO is about 0.43 to 0.67 eV without UV lighting at a temperature below 130 °C. In the UV enhanced experiment, the activation energy is about 0.21 to 0.26 eV at a temperature below 200

Table 1. The activation energy of nano TiO_2 with or without UV enhancement.

Conditions	*Activation Energy*	
	Without UV Enhancement E_a *(eV) (Temperature (°C))*	*With UV Enhancement* E_a*(eV) (Temperature (°C))*
Dry Air	0.35(94<*T*<142)	0.05(94<*T*<232)
80 ppm CO	0.69(94<*T*<124)	0.26(94<*T*<198)
100 ppm CO	0.67(94<*T*<130)	0.21(94<*T*<217)
200 ppm CO	0.43(94<*T*<123)	0.24(94<*T*<199)
300 ppm CO	0.44(94<*T*<127)	0.26(94<*T*<203)

°C that is much lower than that without UV enhancement. These results indicate the UV enhancement of the sensing properties can be interpreted as an increase of the surface activity.

4. CONCLUSIONS

In this study the gas-sensing properties of nano TiO_2 have been demonstrated to be enhanced by UV irradiation. The sensitivity to gaseous CO increases by a factor of 30 with UV light enhancement. The model of photocatalysis can be used to interpret the enhancement of the sensing properties by UV stimulation. Without UV irradiation, the change in the sensitivity is about 0.03/10 ppm of gaseous CO. In the UV enhanced experiment, the change in the sensitivity is about 1.4/10 ppm in range of 80 to 200 ppm of gaseous CO and about 5.3/10 ppm between 200 and 300 ppm of CO. The sensitivity increment indicates that the sensing property with UV assistance is enhanced more than 170 times. The UV enhancement of the gas sensing property can be explained by the decrease of the activity energy of surface reactions.

ACKNOWLEDGEMENTS

We would like to thank the National Science Council, Republic of China for financial support through Contract Number NSC 89-2216-E-036-037.

REFERENCES

[1] Y.K. Chung, M.H. Kim, W.S. Um, H.S. Lee, J.K. Song, S.C. Choi, K.M. Yi, M.J. Lee and K.W. Chung // *Sensors and Actuators B* **60** (1999) 49.

[2] A.R. Phani, S Manorams and V. J. Rao // *Mater Chem. Phys.* **58** (1999) 101.

[3] Y.D. Wang, X.H. Wu and Z.L. Zhou // *Solid-State Electron* **44** (2000) 1603.

[4] N. Savage, B. Chwieroth, A. Ginwalla, B.R. Patton, S.A. Akbar and P.K. Dutta // *Sensors and Actuators B* **79** (2001) 17.

[5] K. Ihokura and J. Watson, *The Stannic Oxide Gas Sensor: Principles and Applications* (CRC Press, Boca Raton, 1994).

[6] M. Schwiezer-Berberich, J.G. Zheng, U. Weimar, W. Göpel, N. Barsan, E. Pentia and A. Tomescu // *Sensors and Actuators B* **31** (1996) 71.

[7] J.I. Yang, H. Lim and S.D. Han // *Sensor and Actuators B* **60** (1999) 71.

[8] N. Hara and K. Sugimoto // *J. Electrochem. Soc.* **137** (1990) 2517.

[9] Y. Takao, Y. Iwanaga, Y. Shimizu and M. Egashira // *Sensors and Actuators* **10** (1993) 229-235.

[10] H. M. Lin, T. Y. Hsu, C. Y. Tung and C. M. Hsu // *Nanostructured Materials* **6** (1995) 1001.

[11] H.-M. Ling, C.-H. Keng and C.-Y. Ttung // *NanoStructured Materials* **9** (1997) 747.

[12] M.C. Carotta, M. Ferroni, D. Gnani, V. Guidi, M. Merli, G. Martinelli, M.C. Casale and M. Notaro // *Sensors and Actuators B* **58** (1999) 310.

[13] N.O. Savage, S.A. Akbar and P.K. Dutta // *Sensors and Actuators B* **72** (2001) 239.

[14] N. Savage, B. Chwieroth, A. Ginwalla, B.R. Patton, S.A. Akbar and P.K. Dutta // *Sensors and Actuators B* **79** (2001) 17.

[15] A. Ruiz, J. Arbiol, A. Cirera, A. Cornet and J.R. Morante // *Materials Science and Engineering C* **19** (2002) 105.

[16] H.D. Jang, S.-K. Kim and S.-J. Kim // *Journal of Nanoparticle Research* **3** (2001) 141.

[17] A. Fujishima and K. Honda // *Nature* **37** (1972) 238.

[18] A. Fujishima, T.N. Rao and D.A. Tryk // *Journal of Photochemistry and Photobiology C*: Photochemistry Reviews **1** (2000) 1.

[19] *Photochemical Conversion and Storage of Solar Energy*, ed. by E. Pelizetti and M. Schiavello (Kluwer Academic Publishers, Dordrecht, 1991).

[20] *Photocatalysis and Environment*, ed. by Schiavello (Kluwer Academic Publishers, Dordrecht, 1988).

[21] K.E. Karakitsou and X.E. Verykios // *J. Phys. Chem.* **97** (1993) 118.

[22] H.D. Jang, S.-K. Kim and S.-J. Kim // *Journal of Nanoparticle Research* **3** (2001) 141.

[23] N. Barsan, M. Schweizer-Berberich and W. Göpel // *Fresenius Journal Analytical Chemistry* **365** (1999) 287.